D. G. Harlow

T. J. Delph

Department of Mechanical Engineering and Mechanics, Lehigh University, Bethlehem, PA 18015

A Probabilistic Model for Creep-Fatigue Failure

We outline here a method for incorporating the scatter observed in creep rupture times and fatigue cycles-to-failure into a probabilistic model for creep-fatigue failure. We do this within the context of the well-known damage fraction summation rule. Various numerical methods for calculating the probability of failure for given creep-fatigue loading cycles are discussed.

1 Introduction

Creep-fatigue damage has long been recognized as one of the principal damage mechanisms in high-temperature pressure vessel and piping systems. Accordingly, it has been the focus of extensive study, and a variety of predictive models for creep-fatigue failure have been developed; e.g., Manson et al. (1971), Pohlemus et al. (1972), Majumdar and Maiya (1980), Yamaguchi and Nishijima (1986), and Gomuc and Bui-Quoc (1986). Without exception, these models have been of a deterministic nature. However, it is well known that both pure fatigue and pure creep failure behavior show marked amounts of scatter in the number of cycles-to-failure at a given strain range (Sinclair and Dolan, 1953; Schijve, 1994), and in the time-to-failure at a given stress level (Garofalo et al., 1961; Farris et al., 1990), respectively. Hence, it is reasonable to infer that failure data under replicated creep-fatigue loading would show a similar degree of scatter, although to the authors' knowledge, there exists little, if any, experimental data to support this inference.

The purpose of the present paper is to indicate how the scatter in fatigue and creep failure data may be incorporated into existing models for creep-fatigue failure prediction to yield the probability of failure for a given loading history. We will do this in the context of what is perhaps the simplest and most widely used of the creep-fatigue failure prediction models, the well-known damage fraction summation rule for creep and fatigue damage, which has been incorporated into the Boiler and Pressure Vessel Code (Code Case N-47) of The American Society of Mechanical Engineers (ASME). However, the methods which we will outline here, based upon well-known concepts from reliability theory, may be equally well applied to other, more complicated, models.

We begin by briefly describing the creep-fatigue damage fraction summation rule. In its most general form, this model assumes the fatigue damage F to be given by Miner's law, as $F = \Sigma_{i=1}^{k} n_i/N_i$, where n_i is the number of cycles at strain range $\Delta\epsilon_i$, and N_i is the number of cycles to failure at this strain range. Likewise, for piecewise-constant stress histories, the creep damage C is assumed to be given by the time-fraction, or Robinson's, rule, in the form $C = \Sigma_{j=1}^{l} t_j/T_j$, where t_j is the creep time at stress level σ_j, and T_j is the time-to-failure at this stress level. The damage summation rule then postulates the existence of a function $F = g(C)$ which defines the creep-fatigue failure envelope on C, F-axes. Combinations of F and C for which $F < g(C)$ would not, according to the damage fraction summation rule, be expected to lead to creep-fatigue failure, whereas failure would be predicted whenever $F > g(C)$. In order that the resulting failure relationship agree with Miner's and Robinson's laws in the case of pure fatigue, or pure creep, respectively, we have $g(0) = 1$ and $g(1) = 0$. Otherwise, $g(C)$ is to be determined from experimental creep-fatigue failure data. Figure 1 shows a bilinear form for $g(C)$, a form which is often used within the context of the ASME Code.

As we have noted, replicated experimental data for the quantities N_i and T_j exhibit considerable amounts of scatter. Hence, it seems reasonable to take the point of view that the quantities N_i and T_j are random variables, for which the probability density functions (pdf's), $f_{N_i}(n_i)$ and $f_{T_j}(t_j)$, may be determined from experimental data. If this is the case, the prediction of creep-fatigue failure becomes inherently a probabilistic problem. One may then seek to calculate the probability that failure will occur after a total creep time t and after a total number of fatigue cycles n, where $t = \Sigma_{j=1}^{l} t_j$ and $n = \Sigma_{i=1}^{k} n_i$. We will discuss three techniques for accomplishing this, one based upon the numerical integration of exact relations from probability theory, the second upon the well-known Monte Carlo technique, and the third upon the second-order reliability method (SORM).

2 Numerical Integration

We first consider the derivation of an exact expression for the failure probability. Analytically, it is somewhat simpler to deal with the survival probability, which is related quite simply to the failure probability by $\Pr\{\text{survival}\} \equiv \Pr\{S\} = 1 - \Pr\{\text{failure}\}$. The survival probability is equal to the probability that the points C, F lie within the region $\mathcal{A}$ in Fig. 1, or $\Pr\{S\} = \Pr\{(C, F) \in \mathcal{A}\}$. Let $f_{\mathbf{T},\mathbf{N}}(\mathbf{t}, \mathbf{n})$ be the joint probability density function (jpdf) for T and N, where we use the standard notation that upper-case variables denote the random variables themselves, whereas lower-case variables denote the variables in the jpdf and $\mathbf{T} = (T_1, T_2, \ldots, T_l)$, etc. Then the probability of survival can be computed directly in terms of the underlying random variables T_j and N_i by

$$\begin{aligned}
\Pr\{S\} &= \Pr\{(C, F) \subset \mathcal{A}\} \\
&= \Pr\{0 < C \le 1, 0 < F \le g(C)\} \\
&= \Pr\left\{0 < \sum_{j=1}^{l} \frac{t_j}{T_j} \le 1, 0 < \sum_{i=1}^{k} \frac{n_i}{N_i} \le g\left(\sum_{j=1}^{l} \frac{t_j}{T_j}\right)\right\} \\
&= \Pr\{a_1 \le T_1 < \infty, \ldots, a_l \le T_l < \infty, \\
&\quad b_1 \le N_1 < \infty, \ldots, b_k \le N_k < \infty\} \\
&= \int_{a_1}^{\infty} \cdots \int_{a_l}^{\infty} \int_{b_1}^{\infty} \cdots \int_{b_k}^{\infty} f_{\mathbf{T},\mathbf{N}}(\tau_1, \ldots, \tau_l, \\
&\qquad \nu_1, \ldots, \nu_k) d\nu_k \ldots d\nu_1 d\tau_l \ldots d\tau_1 \quad (1)
\end{aligned}$$

Contributed by the Pressure Vessels and Piping Division for publication in the JOURNAL OF PRESSURE VESSEL TECHNOLOGY. Manuscript received by the PVP Division, August 1, 1995; revised manuscript received April 25, 1996. Associate Technical Editor: W. K. Liu.

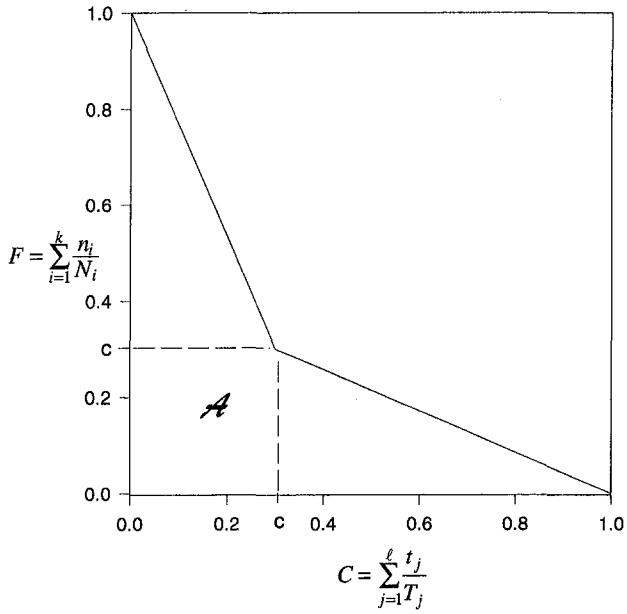

Fig. 1 Bilinear form for creep-fatigue failure function

where

$$a_i = \frac{t_i}{1 - \sum_{j=1}^{i-1} \frac{t_j}{\tau_j}}; \quad b_i = \frac{n_i}{g\left(\sum_{j=1}^{l} \frac{t_j}{\tau_j}\right) - \sum_{j=1}^{i-1} \frac{n_j}{\nu_j}} \tag{2}$$

In almost all cases, the integral in Eq. (1) must be evaluated numerically.

We now give an example based upon experimental creep and fatigue failure data for AISI Type 316 stainless steel, for which sufficient data exist to allow the estimation of the required jpdfs. For this material, the boundaries of the creep-fatigue failure envelope, as given by the ASME Code, have the bilinear form shown in Fig. 1, with the value of c being approximately 0.3.

In order to calculate the survival probability, we need first to specify the jpdfs for the failure times at the desired stress levels and for the number of cycles to failure at the desired strain ranges. Figure 2 shows three sets of replicated uniaxial stress creep rupture data at 1100°F (593°C) at three different stress levels for AISI Type 316 stainless steel, taken from the work of Garofalo et al. (1961). At each stress level, the data are scattered by approximately a factor of 2. When plotted on log-normal probability paper, the data sets can be seen to fall roughly along straight lines, indicating that the scatter in the rupture times at a given stress level can be reasonably well-represented by a log-normal distribution. Hence, we will assume that the jpdf for the creep failure times at differing stress levels is jointly log-normally distributed.

It is analytically more convenient to work with the simpler joint normal distribution, so we define new random variables by $U_j = \ln T_j$, where the T_j are the random failure times at the jth stress level. Then, the U_j will be jointly normally distributed, with jpdf

$$f_{\mathrm{U}}(u_1, \ldots, u_l) = \frac{1}{(2\pi)^{l/2} \det(\mathbf{G})} \exp[-\tfrac{1}{2}\mathbf{p}^T\mathbf{G}^{-1}\mathbf{p}] \tag{3}$$

where $\mathbf{p}^T = (u_1 - \mu_1, \ldots, u_l - \mu_l)$, μ_j is the expected value of U_j, the matrix $\mathbf{G}$ is the variance-covariance matrix for the U_j, and $\det(\mathbf{G})$ denotes the determinant of $\mathbf{G}$. Both μ_j and $\mathbf{G}$ may be estimated from the statistics of the logarithms of the failure times.

Fatigue failure data often seem likewise to be log-normally distributed (Schijve, 1994), although there do not, to our knowledge, exist enough replicated data for Type 316 stainless steel to support the assumption of log-normality for this particular material. It seems reasonable, however, to make this assumption. Hence, if we define $V_i = \ln N_i$, where the N_i are the random cycles-to-failure at the ith strain range, then we will assume the jpdf for the V_i to have the form

$$f_{\mathrm{V}}(v_1, \ldots, v_k) = \frac{1}{(2\pi)^{k/2} \det(\mathbf{H})} \exp[-\tfrac{1}{2}\mathbf{q}^T\mathbf{H}^{-1}\mathbf{q}] \tag{4}$$

where the quantities in Eq. (4) are defined analogously to those in Eq. (3).

The estimation of the statistical parameters required by Eq. (4) is somewhat problematic, given the apparent sparsity of replicated fatigue failure data for Type 316 stainless steel. We have very roughly estimated the required parameters from a nonarchival data set consisting of two cycles-to-failure values, taken at 1100°F (593°C), at each of three strain ranges, $\Delta\epsilon$ = 0.35, 0.40, and 0.60 percent. The corresponding values for the mean and standard deviations of the logarithms of the cycles-to-failure are (14.84, 0.47), (12.85, 0.24), and (9.41, 0.48). The two data points at each strain range do not suffice to allow a determination of the correlation coefficients for the data sets, and here we have assumed values of the correlation coefficient of 0.75 between the data sets at 0.35, 0.40 and 0.40, 0.60 percent, and a value of 0.50 between the data sets at 0.35, 0.60 percent.

Finally, we will assume that $\mathbf{U}_j$ and $\mathbf{V}_i$ are *independent* random vectors. This implies that the jpdf for the failure times and the cycles-to-failure has the form

$$f_{\mathrm{U,V}}(u_1, \ldots, u_l, v_1, \ldots, v_k) = f_{\mathrm{U}}(u_1, \ldots, u_l) f_{\mathrm{V}}(v_1, \ldots, v_k) \tag{5}$$

We subsequently shall have more to say about the validity of this assumption. At the moment, we will simply note that it considerably simplifies the ensuing calculations.

The jpdf $f_{\mathrm{U,V}}$ is related to $f_{\mathrm{T,N}}$ by the change-of-variables theorem (Elishakoff, 1983), which states that

$$f_{\mathrm{T,N}}(t_1, \ldots, t_l, n_1, \ldots, n_k) = |J| f_{\mathrm{U,V}}(u_1, \ldots, u_l, v_1, \ldots, v_k) \tag{6}$$

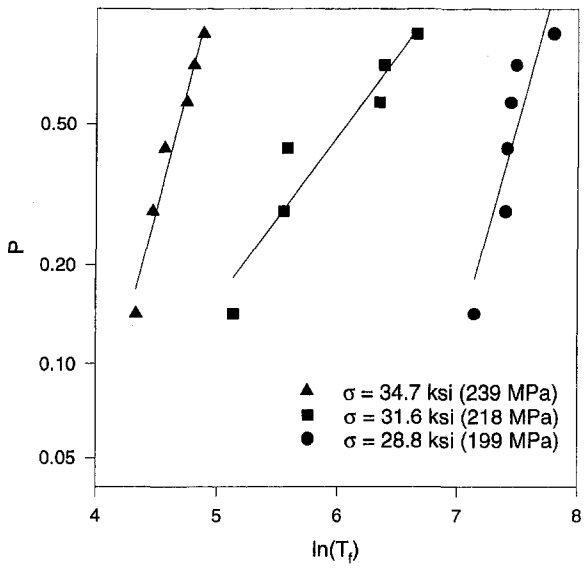

Fig. 2 Creep rupture data plotted on log-normal paper

where $\|$ denotes the absolute value, and J is the Jacobian determinant associated with the change in variables, i.e.,

$$J = \begin{vmatrix} \frac{\partial U_1}{\partial T_1} & \cdots & \frac{\partial U_1}{\partial N_k} \\ \cdots & \cdots & \cdots \\ \frac{\partial V_k}{\partial T_1} & \cdots & \frac{\partial V_k}{\partial N_k} \end{vmatrix} = \frac{1}{T_1 \ldots T_l N_1 \ldots N_k} \quad (7)$$

Hence, from Eqs. (1), (5)–(7), we have

$$\Pr\{S\} = \int \ldots \int f_U(\ln \tau_1, \ldots, \ln \tau_l) \times f_V(\ln \nu_1, \ldots, \ln \nu_k) \frac{d\nu_k \ldots d\nu_1 d\tau_l \ldots d\tau_1}{\tau_1 \ldots \tau_l \nu_1 \ldots \nu_k} \quad (8)$$

We now consider a simple creep-fatigue loading history consisting of periods of constant stress creep at $\sigma = 28.9$ ksi (199 MPa) and of pure fatigue cycling at a strain range of $\Delta\epsilon = 0.30$ percent. Let $X = 1/T$ and $Y = 1/N$. In this case, Eqs. (3)–(4) and (8) lead to the following expression for the probability of survival after a total creep time t at stress level σ and a total of n cycles at a strain range $\Delta\epsilon$ as:

$$\Pr\{S\} = \int_0^{c/t} \int_0^{(1/n)(1-\alpha tx)} f_{X,Y}(x, y)\,dy\,dx + \int_{c/t}^{1/t} \int_0^{(1/an)(1-tx)} f_{X,Y}(x, y)\,dy\,dx \quad (9)$$

where

$$f_{X,Y}(x, y) = \frac{1}{2\pi\eta_\sigma\eta_\epsilon x^2 y^2} \exp\left\{-\frac{1}{2}\left(\frac{\ln\left(\frac{1}{x}\right) - \mu_\sigma}{\eta_\sigma}\right)^2\right\} \times \exp\left\{-\frac{1}{2}\left(\frac{\ln\left(\frac{1}{y}\right) - \mu_\epsilon}{\eta_\epsilon}\right)^2\right\} \quad (10)$$

and $\alpha = (1 - c)/c$. Here μ_σ and μ_ϵ are, respectively, the mean values of the logarithms of the failure times and the cycles-to-failure at the indicated stress and strain range levels, while η_σ and η_ϵ are the corresponding standard deviations of the logarithmic values.

The integrals in Eq. (9) were evaluated using standard numerical integration techniques. The results are shown in Fig. 3,

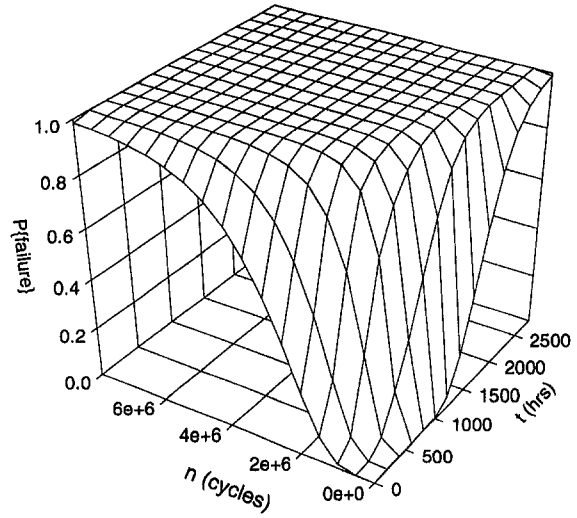

Fig. 3 Failure surface for one creep period and cycling at one strain range

plotted in terms of failure probability as a function of creep time t and number of fatigue cycles n. Not unexpectedly, the combined effects of creep and fatigue act to substantially increase the failure probability in comparison to the cases of pure creep or pure fatigue.

3 Monte Carlo Simulation

A rapid and simple alternative to the numerical evaluation of the failure probability is the well-known Monte Carlo technique, which we will briefly describe in the context of the present problem. This method has the attractive feature that it completely avoids numerical evaluation of integrals of the sort described in the previous section, but instead works directly with the basic equation defining the creep-fatigue failure envelope

$$\sum_{i=1}^{k} \frac{n_i}{N_i} = g\left(\sum_{j=1}^{l} \frac{t_j}{T_j}\right) \quad (11)$$

In a single Monte Carlo simulation, one generates a total of k random cycles-to-failure N_i and l random failure times T_j, using a random number generator. Then, for given values of n_i and t_j, failure occurs whenever

$$\sum_{i=1}^{k} \frac{n_i}{N_i} > g\left(\sum_{j=1}^{l} \frac{t_j}{T_j}\right) \quad (12)$$

This process is repeated a large number of times, with the probability of failure being estimated as the number of instances of failure divided by the total number of simulations.

As an example, we consider a situation with three creep hold periods, and three periods of fatigue cycling. For the creep periods, 50 percent of the total creep time t was assumed to be spent at a stress level of $\sigma_1 = 28.9$ ksi (199 MPa), 30 percent at $\sigma_2 = 31.6$ ksi (218 MPa), and the remaining 20 percent at $\sigma_3 = 34.7$ ksi (239 MPa). Likewise, 60 percent of the total number of cycles n were assumed to be spent at a strain range of $\Delta\epsilon_1 = 0.35$ percent, with 20 percent at $\Delta\epsilon_2 = 0.40$ percent and 20 percent at $\Delta\epsilon_3 = 0.60$ percent.

Each Monte Carlo simulation requires two triplets of random numbers, (T_1, T_2, T_3) and (N_1, N_2, N_3). These were obtained by using a normal (Gaussian) random number generator to generate triplets (X_1, X_2, X_3) of independent, normally distributed random numbers with zero mean and unit variance. To obtain from these, for example, three random failure times (T_1, T_2, T_3) which are jointly log-normally distributed, we take, as before, $\mathbf{p}^T = (U_1 - \mu_1, U_2 - \mu_2, U_3 - \mu_3)$, where $U_i = \ln(T_i)$ and μ_i is the expected, or mean value of $\ln(T_i)$. Now introduce the change of variables $\mathbf{p} = \mathbf{ZY}$, where $\mathbf{Y}^T = (Y_1, Y_2, Y_3)$, and $\mathbf{Z}$ is the matrix whose columns are the eigenvectors of $\mathbf{G}$. Then we may write the quadratic form appearing in Eq. (3) as

$$\mathbf{p}^T\mathbf{G}^{-1}\mathbf{p} = \frac{Y_1^2}{\alpha_1} + \frac{Y_2^2}{\alpha_2} + \frac{Y_3^2}{\alpha_3} \quad (13)$$

where $(\alpha_1, \alpha_2, \alpha_3)$ are the eigenvalues of the variance-covariance matrix $\mathbf{G}$. Hence, (Y_1, Y_2, Y_3) are normally distributed, independent random numbers with zero mean and variance $(1/\alpha_1, 1/\alpha_2, 1/\alpha_3)$, and we may write $(Y_1, Y_2, Y_3) = (X_1/\sqrt{\alpha_1}, X_2/\sqrt{\alpha_2}, X_3/\sqrt{\alpha_3})$. A similar procedure yields the three random cycles-to-failure (N_1, N_2, N_3).

The results are shown in Fig. 4, where, again, we plot the probability of failure versus total creep time t and total number of cycles n. Each point on the plot was the result of 5000 Monte Carlo trials. Figure 4 is qualitatively similar to Fig. 3. Quantitatively, the probability of failure at a given time and/or number of cycles has been increased from that shown in Fig. 3, due to the presence of creep hold times at higher stress levels and fatigue cycling at higher strain ranges.

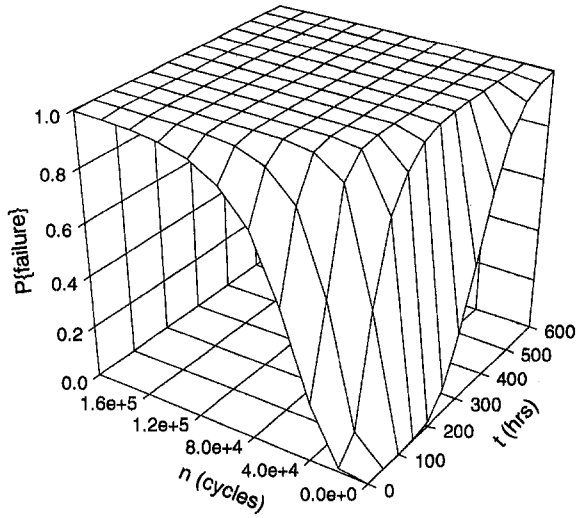

Fig. 4 Failure surface for creep at three stress levels and fatigue at three strain ranges

4 Second-Order Reliability Method

Here we briefly outline the second-order reliability method (SORM) and describe how it is applied to the problem at hand. SORM is an approximate technique for the solution of reliability problems which has found wide use in various applications. As we shall discuss later, the approximation improves as the probability of failure decreases. A good general description of the technique is given by Madsen et al. (1986).

In general, the first step is to express the failure function $F = g(C)$ in terms of standard independent normal variables $X_1, \ldots, X_{k+l}$. From the analysis in the previous sections, we may write, for example,

$$\ln(T_1) = \frac{G_{11}X_1}{\sqrt{\alpha_1}} + \frac{G_{12}X_2}{\sqrt{\alpha_2}} + \ldots + \frac{G_{1l}X_l}{\sqrt{\alpha_l}} + \mu_1 \quad (14)$$

where $\mu_1 = E(\ln T_1)$, and $E(\ )$ denotes the expected value. The failure function thus becomes

$$\sum_{i=1}^{k} n_i e^{-\mu_{l+i}} \prod_{j=1}^{k} e^{-H_{ij}X_{l+j}/\sqrt{\gamma_j}} = g\left(\sum_{i=1}^{l} t_i e^{-\mu_i} \prod_{j=1}^{l} e^{-G_{ij}X_j/\sqrt{\alpha_j}}\right) \quad (15)$$

where $\mu_{l+j} = E(\ln N_j)$ and the quantities γ_j are the eigenvalues of the matrix $\mathbf{H}$. One then seeks the *failure point* $\mathbf{X}^*$, which is defined as the point on the failure surface in the space of the variables X_i, defined by Eq. (15), which has minimum distance $\beta = \sqrt{\sum_{i=1}^{k+l} X_i^{*2}}$ to the origin. The region about this point may be expected to make the largest contribution to the integral for the failure probability. This point may be determined using standard constrained minimization techniques, e.g., Schittkowski (1986), the constraint being that the point lies on the failure surface. However, in the present case, it was found to be simpler to utilize (15) to numerically determine the value of one of the variables in terms of the values of the remaining $k + j - 1$ variables, thus resulting in an unconstrained minimization problem.

Let the failure surface given by (15) be denoted by $h(X_i) = 0$, defined so that the region $h(X_i) > 0$ corresponds to the safe region. Further, let $X_i^* = \beta b_i$, so that $\mathbf{b}$ is a unit vector from the origin to the failure point. The failure surface in the neighborhood of the failure point is then approximated by a parabolic surface obtained by Taylor series expansion about the failure point. To accomplish this, we construct the $(k + l) \times (k + l)$ orthonormal matrix $\mathbf{H}$ whose last column is the vector $\mathbf{b}$, and introduce the change of coordinates

$$X_i = H_{ij}Y_j + \beta b_i \quad (16)$$

where the summation convention for repeated subscripts is implied. With this transformation, the origin of the Y-coordinate system lies at the failure point, with the Y_n coordinate normal to the failure surface. Then, the equation for the failure surface becomes

$$h(H_{ij}Y_j + \beta b_i) = 0 \quad (17)$$

which implicitly defines $Y_n = f(Y_1, Y_2, \ldots, Y_{n-1})$. Because Y_n is normal to the failure surface, $Y_1, Y_2, \ldots, Y_{n-1}$ must lie in the tangent plane. This implies that, at the failure point

$$\frac{\partial Y_n}{\partial Y_1} = \frac{\partial Y_n}{\partial Y_2} = \ldots = \frac{\partial Y_n}{\partial Y_{n-1}} = 0 \quad (18)$$

Hence, by Taylor series expansion in the neighborhood of the failure point

$$Y_n = f(Y_1, Y_2, \ldots, Y_{n-1}) = \frac{1}{2}\frac{\partial^2 f}{\partial Y_i \partial Y_j} Y_i Y_j + \ldots \quad (19)$$

for $i, j = 1, \ldots, k + l - 1$. Again, the summation convention is implied, and the second derivative in Eq. (19) is evaluated at the point $Y_1 = \ldots Y_{k+l-1} = 0$. From Eq. (17), we have that $\partial^2 h/\partial Y_i \partial Y_j = 0, i, j = 1, \ldots, k + l - 1$, and this, in conjunction with Eqs. (16) and (18), leads to

$$F_{mn} \equiv \frac{\partial^2 f}{\partial Y_m \partial Y_n} = -\frac{D_{ij}H_{im}H_{jn}}{g_i H_{in}} \quad (20)$$

where the range of summation over the indices i and j is $1 \rightarrow k + l$, but $m, n = 1, \ldots, k + l - 1$. Here $g_i = (\partial h/\partial X_i)|_{\mathbf{x}=\mathbf{x}^*}$ and $\mathbf{D}$ is the matrix whose entries are the second-order partial derivatives evaluated at the failure point, i.e.,

$$D_{ij} = \left.\frac{\partial^2 h}{\partial X_i \partial X_j}\right|_{\mathbf{x}=\mathbf{x}^*} \quad (21)$$

Truncating Eq. (19) at the first term, we have

$$Y_n \approx \tfrac{1}{2}F_{ij}Y_iY_j \quad (22)$$

The principal curvatures κ_i, $i = 1, 2, \ldots, k + l - 1$ of the parabolic approximation to the failure surface given by Eq. (22) are simply the eigenvalues of $\mathbf{F}$. With this approximation, it becomes possible to derive asymptotic estimates for the probability integral (Tvedt, 1983; Breitung, 1984), or to rewrite the probability integral in a form suitable for efficient numerical evaluation (Tvedt, 1988). Then, a three-term approximation to the failure probability is (Tvedt, 1983; Breitung, 1984)

$$\Pr\{\text{failure}\} = A_1 + A_2 + A_3 \quad (23)$$

where

$$A_1 = \Phi(-\beta) \prod_{j=1}^{k+l-1} (1 + \beta\kappa_i)^{-1/2} \quad (24)$$

$$A_2 = [\beta\Phi(-\beta) - \phi(\beta)] \times \left\{\prod_{j=1}^{k+l-1} (1 + \beta\kappa_i)^{-1/2} - \prod_{j=1}^{k+l-1} (1 + (\beta + 1)\kappa_i)^{-1/2}\right\}$$

$$A_3 = (\beta + 1)[\beta\Phi(-\beta) - \phi(\beta)]\left\{\prod_{j=1}^{k+l-1} (1 + \beta\kappa_i)^{-1/2} - \mathrm{Re}\left[\prod_{j=1}^{k+l-1} (1 + (\beta + i)\kappa_i)^{-1/2}\right]\right\} \quad (25)$$

and $\Phi(\ )$ is the standard normal cumulative distribution function, and $\phi(\ )$ the corresponding standard normal density function.

Alternatively, an exact integral formulation for the failure probability computed from the parabolic approximating surface has been given by Tvedt (1988). This is

$$\Pr\{\text{failure}\} = \phi(\beta)\,\mathrm{Re}\left\{ i\sqrt{\frac{2}{\pi}} \int_0^{i\infty} e^{\psi(u)} du \right\} \qquad (26)$$

where

$$\psi(u) = \tfrac{1}{2}(u+\beta)^2 - \ln(u) - \tfrac{1}{2}\sum_{j=1}^{k+l-1} \ln(1-\kappa_j u) \qquad (27)$$

In order to place this in a form suitable for efficient numerical evaluation, the contour of integration is shifted to the left of the origin to the saddle point defined by $\psi'(u_s) = 0$ where $(\ )'$ indicates differentiation with respect to u. Then, with the change of variables $u = u_s + ibv$, where $b = \sqrt{2/\psi''(u_s)}$, Eq. (26) becomes

$$\Pr\{\text{failure}\} = b\phi(\beta)\sqrt{\frac{2}{\pi}} \int_0^{\infty} e^{\mathrm{Re}(\psi)} \cos(\mathrm{Im}(\psi))\, dv \qquad (28)$$

In this form, the integral is especially suited to trapezoidal rule evaluation.

Figure 5 shows some results for the case considered in Fig. 3, with the probability of failure according to the SORM approximation computed along the intersection of the surface shown in Fig. 3 with the plane $n = 2500t$. Also shown are results obtained from numerical integration and Monte Carlo simulation. The Monte Carlo simulations show the 99 percent confidence bounds corresponding to each value of t, constructed by carrying out 100 separate simulations of 10^6 trials each. Although the Monte Carlo bounds are quite tight for higher probabilities of failure, they become increasingly wide with decreasing probability of failure, with the lower bound tending to zero for sufficiently small values of t. The results from numerical integration diverge from the SORM and Monte Carlo results for small values of t. Because SORM is known to be asymptotically exact for small failure probabilities, this is likely an indication of increasing error in the numerical integration as the probability of failure decreases. Figure 6 shows similar results for the case considered in Fig. 4, computed along the intersection of the surface with the plane $n = 50t$. Here, the Monte Carlo simulations predicts zero failure probability for sufficiently small values of t. In most cases considered, the SORM failure probabilities computed from Eq. (28) were found to differ by less than 1 percent from those computed by the asymptotic approximation given by Eqs. (23)–(24).

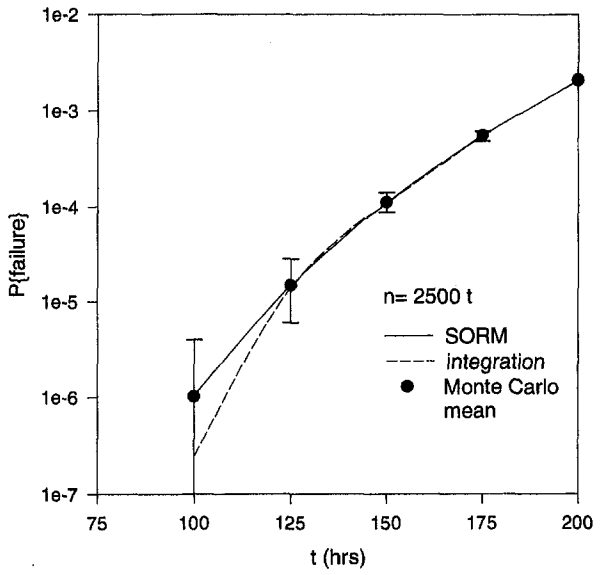

Fig. 5 Results from exact integration, Monte Carlo, and SORM for one creep stress level, one fatigue strain range

5 Discussion

In the foregoing, we have demonstrated how the very marked scatter present in creep rupture times-to-failure and in fatigue cycles-to-failure may be taken into account in constructing probabilistic models of creep-fatigue failure. Because it is the simplest and most widely used, although not necessarily the best, of the available creep-fatigue failure models, we have chosen to do this in the context of the damage fraction summation model incorporated into the ASME Code. We have presented three methods for determining the probability of survival under creep-fatigue conditions, one based upon numerical integration of the probability integral, another upon Monte Carlo simulation, and the third upon the second-order reliability method (SORM).

The accuracy of the formulation based upon the exact probability integral is limited only by the accuracy of the numerical techniques used to evaluate the multiple integrals involved in the expression for the failure probability. However, the computational effort required for the numerical evaluation of these integrals rises rapidly with the number of random variables, and becomes prohibitive if more than four or so integrations are required. In the present case, it was found not to be possible to compute in a reasonable time the sixfold probability integral for the examples shown in Figs. 4 and 6. Thus, this technique is usable only with a relatively small number of creep hold times at different stress levels and/or fatigue periods at different strain ranges. In addition, the results appear to become less accurate as the failure probabilities become smaller.

In contrast, Monte Carlo techniques allow quite rapid estimates of the failure probability to be made for any number of creep/fatigue cycles within the range of practical interest. The accuracy of the estimation, of course, improves with the number of Monte Carlo trials. However, Monte Carlo techniques have the marked disadvantage that the estimates for small values of the failure probability are known to be poor, and may require a prohibitively large number of trials in order to obtain acceptable accuracy. In general, formal statistical tests, such as the confidence bounds we have used here, are required to assess accuracy. Nevertheless, a commonly applied rule-of-thumb is that, to obtain acceptable accuracies for failure probabilities on the order of 10^{-n}, 10^{n+2} Monte Carlo trials are necessary. This is a particular disadvantage in the present case, because, for well-designed pressure vessel and piping systems, the failure probability may expected to be quite low.

Of the three techniques we have outlined here, the second-order reliability method (SORM) appears for several reasons to be best suited to the solution of the probabilistic creep-rupture problem. It is capable of handling with reasonable computational effort realistic numbers of creep hold times at varying stress levels and/or fatigue cycle periods at varying strain ranges. Furthermore, in contrast to Monte Carlo simulation, it yields quite good estimates of the failure probability when the failure probability is small. In fact, it is known (Breitung, 1984) to yield asymptotically exact results in the limit as the failure probability becomes small. Because the failure probability is typically small in most applications, this is the regime of engineering interest.

A drawback in the present case is the lack of a nonsmooth failure surface (Fig. 1). If the SORM failure point should happen to lie at the intersection of the two linear portions of the surface, then SORM is inapplicable, because it requires the

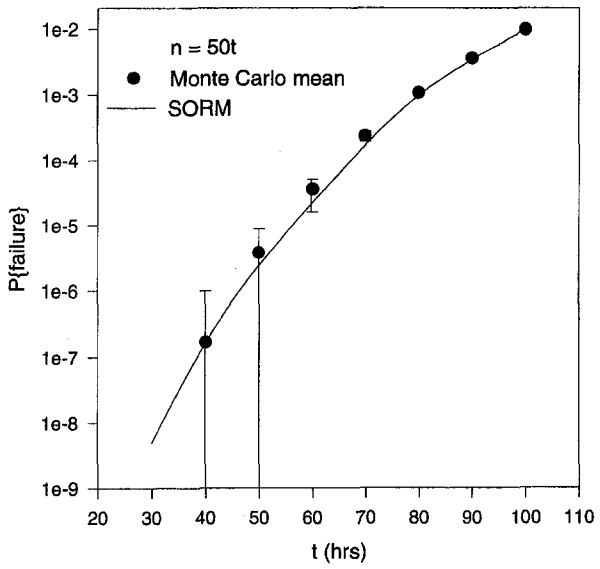

Fig. 6 Monte Carlo and SORM results for three creep stress levels and three fatigue strain ranges

existence of continuous second derivatives at this point. However, the bilinear failure surface merely represents a convenient fit to the experimental creep-fatigue failure data, and this problem could be avoided by refitting the data with a sufficiently smooth function.

Figure 5 shows a comparison of results obtained by the three methods outlined here for the case treated in Fig. 3, with creep at a single stress level interspersed with periods of fatigue cycling at a single strain range. It can be seen that for failure probabilities down to about 10^{-5}, the predictions of the three methods agree quite well. For probabilities below this value, the results from the numerical integration fall below the predictions of the other two methods, probably due to increasing numerical error. Additionally, the confidence bounds on the Monte Carlo simulations begin to widen markedly, with the lower bound eventually falling to zero. This illustrates the tendency of the Monte Carlo method to perform poorly at low failure probabilities. Figure 6 shows similar results for the case treated in Fig. 4, with creep at three different stress levels and fatigue cycling at three different strain ranges. In this latter case, it was found to be computationally infeasible to numerically compute the sixfold multiple integral expression for the failure probability, and only Monte Carlo and SORM results are shown. Here the SORM results agree quite well with the Monte Carlo mean values for failure probabilities down to $10^{-6} - 10^{-7}$, although the confidence bounds at these levels become quite wide. For failure probabilities less than about 10^{-7}, however, the Monte Carlo method with 10^8 trials predicts zero probability of failure. Increasingly large numbers of trials would be required to obtain accurate results at these low probability levels.

In the foregoing, we have assumed that the stress and strain range histories are piecewise constant, and have not attempted to treat the more considerably more complicated case of continuously varying stress and/or strain range histories. We will, however, sketch out the primary considerations here. For definiteness, suppose that the stress history is continuously time-varying, given by $\sigma(t)$. Then the time-fraction rule for creep damage generalizes to

$$C = \int_0^t \frac{d\tau}{T(\sigma(\tau))} \tag{29}$$

where $T(\sigma)$ denotes the random failure time at stress level σ. Thus, T becomes a stochastic process, indexed by the stress level σ. One may reasonably assume that the process is stationary. In order to completely specify the process, the autocorrelation function for the process must be known, which must be estimated from experimental data. In general, when stochastic processes are involved, estimations of failure probabilities are much more difficult to obtain, and techniques for doing so are not as well developed as for the case we have considered here. The SORM technique, for example, is applicable only in certain limited circumstances, and Monte Carlo simulation becomes much more complicated.

Although we have chosen to present the probabilistic failure prediction techniques outlined here in the context of the simple damage fraction summation rule, they are equally applicable to more sophisticated, and presumably more accurate, creep-fatigue failure prediction models, such as those cited in the References. The damage fraction summation model is well known to lead to systematically inaccurate failure predictions in certain circumstances, and more complicated models are capable of doing better in this regard. However, the scatter in the experimental data is no less for more complicated models than for simpler models, and this scatter, if not taken into account, is quite capable of overwhelming any increase in predictive ability associated with more sophisticated creep-fatigue failure models.

Perhaps the primary difficulty encountered in trying to make the sort of probabilistic creep-rupture calculations outlined here is not the calculations themselves, but the paucity of experimental data upon which to base the calculations. Replicated sets of creep rupture and fatigue failure data are not plentiful, and replicated creep-fatigue data seem to be almost nonexistent. Obviously, any predictions of the probability of creep-fatigue failure are strongly dependent upon the form of the distributions assumed, and these can be determined only from experimental data. In particular, in the absence of experimental data, we have assumed that the random failure times in creep T_i are independent of the random number of cycles-to-failure in fatigue N_i. However, metallurgical evidence indicates that, at elevated temperatures, low-cycle fatigue and creep damage mechanisms are often quite similar, e.g., intergranular cavitation. Hence, the assumption of independence is quite questionable. Unfortunately, to our knowledge, the experimental data which might link creep and fatigue failure statistically are not available at the present time.

Acknowledgment

This work was supported by the Materials Research Group (MRG) Program of the Division of Materials Research, National Science Foundation under Grant. No. DMR-9102093.

References

Breitung, K., 1984, "Asymptotic Approximations for Multinormal Integrals," ASCE *Journal of Engineering Mechanics,* Vol. 110, pp. 357–366.

Elishakoff, I., 1983, *Probabilistic Methods in the Theory of Structures,* Wiley-Interscience, New York, NY.

Farris, J. D., Lee, J. P., Harlow, D. G., and Delph, T. J., 1990, "On the Scatter in Creep-Rupture Times," *Metallurgical Transactions A,* Vol. 21A, pp. 345–352.

Garofalo, F., Whitmore, R. W., Domis, W. F., and von Gemmingen, F., 1961, "Creep and Creep-Rupture Relationships in an Austenitic Stainless Steel," *Transactions of the Metallurgical Society of the AIME,* Vol. 221, pp. 310–319.

Gomuc, R., and Bui-Quoc, T., 1986, "An Analysis of the Fatigue/Creep Behavior of Type 304 Stainless Steel using a Continuous Damage Approach," ASME JOURNAL OF PRESSURE VESSEL TECHNOLOGY, Vol. 108, pp. 280–288.

Majumdar, S., and Maiya, P. S., 1980, "A Mechanistic Model for Time-Dependent Fatigue," ASME *Journal of Engineering Materials and Technology,* Vol. 102, 159–167.

Manson, S. S., Halford, G. R., and Hirschberg, M. H., 1971, "Creep-Fatigue Analysis by Strain-Range Partitioning," *Design for Elevated Temperature Environment,* eds., S. Y. Zamrik and R. I. Jetter, American Society of Mechanical Engineers, New York, NY, pp. 12–28.

Masden, S. O., Krenk, S., and Lind, N. C., 1986, *Methods of Structural Safety,* Prentice-Hall, Englewood Cliffs, NJ, pp. 65–69.

Polhemus, J. F., Spaeth, C. E., and Vogel, W. H., 1972, "Ductility Exhaustion Model for Predicting Thermal Fatigue and Creep Interaction," *Fatigue at Elevated Temperatures,* ASTM STP-465, A.S.T.M., Philadelphia, PA, pp. 625–635.

Schijve, J., 1994, "Fatigue Predictions and Scatter," *Fatigue and Fracture of Engineering Materials and Structures,* Vol. 17, pp. 381–396.

Schittkowski, K., 1986, "NLPQL: A FORTRAN Subroutine Solving Constrained Nonlinear Programming Problems," *Annals of Operations Research,* Vol. 5, pp. 485–500.

Sinclair, G. M., and Dolan, T. J., 1953, "Effect of Stress Amplitude on Statistical Variability in Fatigue Life of 75S-T6 Aluminum Alloy," TRANS. ASME, Vol. 75, pp. 867–872.

Tvedt, L., 1983, "Two Second-Order Approximations to the Failure Probability," Veritas Report RDIV/20-004-83, Det norske Veritas, Oslo, Norway.

Tvedt, L., 1988, "Second-Order Reliability by an Exact Integral," *Reliability & Optimization of Structural Systems '88,* ed., P. Thoft-Christensen, Springer-Verlag, Berlin, Germany, pp. 377–384.

Yamaguchi, K., and Nishijima, S., 1986, "Prediction and Evaluation of Long-Term Creep-Fatigue Life," *Fatigue and Fracture of Engineering Materials and Structures,* Vol. 9, pp. 96–107.